

Bond-length relaxation in $\text{Si}_{1-x}\text{Ge}_x$ alloys

D. B. Aldrich, R. J. Nemanich, and D. E. Sayers

Department of Physics, North Carolina State University, Raleigh, North Carolina 27695-8202

(Received 3 August 1994)

We have measured and quantified the effect of alloy composition on the atomic bonding in relaxed molecular-beam-epitaxy-deposited crystalline $\text{Si}_{1-x}\text{Ge}_x$ alloys. X-ray-absorption fine structure (XAFS) and x-ray diffraction were used to examine how the atomic bonding in $\text{Si}_{1-x}\text{Ge}_x$ is affected by changes in alloy composition. In this study, the Ge-Ge and Ge-Si bond lengths were measured using XAFS and compared with the conflicting results of existing analytical models and previous XAFS studies. The measured Ge-Ge and Ge-Si bond lengths were found to be in good agreement with the analytical models, which predict that the Ge-Ge, Ge-Si, and Si-Si bonds maintain distinctly different lengths which change linearly with alloy composition. The topological rigidity parameter a^{**} was used to quantify the linear dependence of the bond lengths on alloy composition and a value of $a^{**}=0.63$ was calculated from the measured bond lengths. An extensive XAFS error analysis was performed and the error in the topological rigidity parameter $a^{**}=0.63_{-0.13}^{+0.08}$ was determined. This value of a^{**} , which is notably different from 0 or 1, indicates that both the bond lengths and bond angles are distorted by changes in composition.

I. INTRODUCTION

The use of $\text{Si}_{1-x}\text{Ge}_x$ heterostructures in integrated and photoelectronic devices has been attracting increasing attention. Many studies have been performed to investigate the effects of composition and strain on the electrical properties of $\text{Si}_{1-x}\text{Ge}_x$, but the atomic scale properties of $\text{Si}_{1-x}\text{Ge}_x$ have yet to be adequately determined. While x-ray-absorption fine-structure (XAFS) measurements have proven effective for determining bond lengths in III-V alloys,¹ there have been only limited XAFS experiments to measure directly the atomic bonding in Si-Ge alloys. In fact, there are significant differences between the existing theoretical models and some of the previous XAFS measurements.

The underlying structure of silicon and germanium is the diamond lattice. The natural lattice constant of Ge is 4.2% larger than the natural lattice constant of Si (5.6576 and 5.4309 Å, respectively). Si and Ge are completely soluble, and $\text{Si}_{1-x}\text{Ge}_x$ alloys form continuous solid solutions over the entire composition range ($0 \leq x \leq 1$). The effect of changing composition on the atomic configuration of $\text{Si}_{1-x}\text{Ge}_x$ has been predicted, in the extremes, by Bragg,² Pauling,³ and Vegard.⁴ According to Bragg and Pauling, atomic radii are approximately conserved and, as composition changes, bond lengths remain unchanged. With the bond lengths fixed, the bond angles must distort from the tetrahedral angle to accommodate the presence of different size atoms. Vegard's law assumes the lattice parameters of the alloy are the compositionally weighted average of the natural Si and Ge lattice constants. On the atomic scale it is assumed that all the bonds in the alloy have the same "effective" length. As the composition of the alloy changes, the "effective" bond length changes, and the bond angles remain fixed at

the tetrahedral angle.

Theoretical studies of $\text{Si}_{1-x}\text{Ge}_x$ alloys have indicated that bulk $\text{Si}_{1-x}\text{Ge}_x$ alloys may not strictly adhere to either the Bragg-Pauling or Vegard models. Studies by Martins and Zunger,⁵ Weidmann and Newman,⁶ and Mousseau and Thorpe⁷ all suggest that bond lengths and bond angles change as alloy composition changes. Martins and Zunger⁵ used a valence force field (VFF) approach to calculate symmetric lattice distortions around isovalent impurities. They calculated values of 2.380 and 2.419 Å for the Ge-Si bond length at the Ge and Si impurity limits, respectively. It was theorized that the Ge-Si bond length would vary linearly, with alloy composition, between these two values.⁵ In the studies by Weidmann and Newman⁶ and Mousseau and Thorpe,⁷ relaxed elastic network Si-Ge supercells were used as models of bulk $\text{Si}_{1-x}\text{Ge}_x$ to calculate properties of the alloy. In both studies it was found that Ge-Ge, Ge-Si, and Si-Si bonds maintain distinctly different lengths which vary linearly with alloy composition.

In an analytical study by Cai and Thorpe,⁸ they define a topological rigidity parameter a^{**} which is a measure of the rigidity of the lattice. In the diamond lattices of Si and Ge each atom is bonded to four neighboring atoms. If an atom applies a radial force against its four neighbor atoms, the neighbor atoms will be displaced. The other bonds of the neighbor atoms and the rest of the lattice will partially counteract the applied force and will diminish the displacement. As a^{**} is defined by Cai and Thorpe it is a measure of the force required to produce a unit displacement (force $\propto 1/a^{**}$). For a rigid lattice, $0 \leq a^{**} \leq 0.5$ ($a^{**}=0$ in a perfectly rigid lattice). In a lattice where less force is required to displace the atoms, $0.5 \leq a^{**} \leq 1$ ($a^{**}=1$ is the "floppy" limit). For bulk $\text{Si}_{1-x}\text{Ge}_x$ alloys the definition of the topological rigidity

parameter a^{**} can be reduced to

$$\begin{aligned} L_e &= (1-x)L_{\text{SiSi}}^0 + xL_{\text{GeGe}}^0, \\ \langle L_{\text{SiSi}} \rangle &= L_e - xa^{**}(L_{\text{GeGe}}^0 - L_{\text{SiSi}}^0), \\ \langle L_{\text{GeGe}} \rangle &= \langle L_{\text{SiSi}} \rangle + a^{**}(L_{\text{GeGe}}^0 - L_{\text{SiSi}}^0), \\ \langle L_{\text{GeSi}} \rangle &= \frac{1}{2}(\langle L_{\text{GeGe}} \rangle + \langle L_{\text{SiSi}} \rangle), \end{aligned} \quad (1)$$

where L_{GeGe}^0 and L_{SiSi}^0 are the natural Ge-Ge, and Si-Si bond lengths, respectively, and $\langle L_{\text{GeGe}} \rangle$, $\langle L_{\text{GeSi}} \rangle$, and $\langle L_{\text{SiSi}} \rangle$ are the Ge-Ge, Ge-Si, and Si-Si bond lengths in a bulk $\text{Si}_{1-x}\text{Ge}_x$ alloy of composition x .⁷ The parameter L_e is analogous to the "effective" bond of Vegard's law which varies linearly from the natural bond length of Si-Si to the natural bond length of Ge-Ge as the alloy composition changes from $x=0$ to 1.

The parameter a^{**} can be thought of as a measure of the effect of composition on bond length. In Vegard's limit $a^{**}=0.0$, and the Ge-Ge, Ge-Si, and Si-Si bond lengths are equal to the effective bond length L_e . In the Bragg-Pauling limit $a^{**}=1.0$, and the bond lengths remain at their natural values independent of the alloy composition. For comparison we have determined a^{**} from the results of several previous analytical and experimental studies. From the theoretical results of Weidmann and Newman⁶ we determined, using Eqs. (1), the value of $a^{**}=0.63\pm 0.04$. Mousseau and Thorpe⁷ determined $a^{**}=0.707$ from the bulk $\text{Si}_{1-x}\text{Ge}_x$ Monte Carlo simulations of de Gironcoli, Giannozzi, and Baroni.⁹ From the results of the study of Martins and Zunger⁵ we calculated a value of $a^{**}=0.60\pm 0.03$ for bulk $\text{Si}_{1-x}\text{Ge}_x$. These values of a^{**} ($0.6 \leq a^{**} \leq 0.7$) suggest that atomic bonding does not strictly adhere to the either Vegard model or the Bragg-Pauling model, and that both the bond lengths and bond angle change with composition.

In apparent conflict with these analytical results are the results of an extended x-ray-absorption fine-structure (EXAFS) investigation of $\text{Si}_{1-x}\text{Ge}_x$ by Kajiyama *et al.*¹⁰ which indicated that the bond lengths in $\text{Si}_{1-x}\text{Ge}_x$ alloy exhibit Bragg-Pauling-type behavior. In the study of Kajiyama *et al.* the Ge-Ge and Ge-Si bond lengths measured for samples ranging in composition from $x=0.20$ to 1.00 varied only slightly with composition. We determined a value of $a^{**}=0.98$ from the Ge-Ge and Ge-Si bond lengths measured by Kajiyama *et al.*

This study addresses the apparent conflict between the theoretical predictions and previous experimental observations of atomic bonding in bulk $\text{Si}_{1-x}\text{Ge}_x$ alloys. Careful attention has been given to two problem areas of previous studies: sample preparation and EXAFS error analysis. Samples were prepared in ultrahigh vacuum and their composition, purity, and crystallinity were checked by several techniques. The EXAFS error analysis included the examination of many possible sources of error. Each source of error was identified and examined to determine the magnitude of its contribution to the error in the measured bond length. The total error was determined by summing the contributions of all the individual sources of error.

II. EXPERIMENT

To examine the effect of composition on atomic bonding, $\text{Si}_{1-x}\text{Ge}_x$ layers of differing composition were deposited on Si(100) substrates. The molecular-beam epitaxy (MBE) deposited $\text{Si}_{1-x}\text{Ge}_x$ alloys were grown on clean Si(100) substrates at 550°C. The Si wafers were pre-cleaned by (1) exposure to UV-generated ozone to remove hydrocarbons from the surface and to form a stable silicon oxide, (2) spin etching with a solution of hydrofluoric acid: deionized H_2O : ethanol (1:1:10) to remove the silicon oxide and leave a hydrogen terminated surface, and (3) *in situ* thermal desorption at > 850°C for 10 min to remove any remaining surface contaminants. This cleaning process has been shown to produce atomically clean surfaces.¹¹ Following an *in situ* thermal desorption at > 850°C, the substrate temperature was reduced and held at 550°C for deposition of a homoepitaxial silicon buffer layer (225 Å) and a heteroepitaxial $\text{Si}_{1-x}\text{Ge}_x$ alloy layer (> 2000 Å). The processing chamber base pressure was $\sim 1 \times 10^{-10}$ Torr, desorption pressure was $< 5 \times 10^{-10}$ Torr, and deposition pressure was $< 5 \times 10^{-8}$ Torr. Silicon and germanium were codeposited from two electron-beam evaporation sources. The Si and Ge deposition rates were monitored using oscillating quartz-crystal monitors. Feedback from the deposition monitors was used to control automatically the relative Si and Ge deposition rates, and the maximum composition variation during deposition was $\approx 2\%$.

When crystalline $\text{Si}_{1-x}\text{Ge}_x$ is deposited on a substrate, the substrate will exert an influence on the alloy. The most studied case of this effect is that of $\text{Si}_{1-x}\text{Ge}_x$ on a Si substrate. Silicon-germanium alloys can be formed in a strained state when grown on Si(100).¹² The $\text{Si}_{1-x}\text{Ge}_x$ alloy lattice parameters parallel to the $\text{Si}_{1-x}\text{Ge}_x/\text{Si}$ interface are initially compressed to match the Si substrate (pseudomorphic growth). The biaxial compression at the interface distorts the atomic bonding, increases the internal strain energy, and causes the alloy lattice to expand uniaxially in the direction normal to the alloy/substrate interface.¹³ As the thickness of the alloy increases, the total internal strain energy of the alloy increases. When the internal strain energy is greater than the strength of the bonds at the alloy/Si interface, some interface bonds are broken (defect formation) allowing the compressed alloy lattice parameters to expand (relaxation).¹³ A strained $\text{Si}_{1-x}\text{Ge}_x$ alloy can also be relaxed by increasing the amount of thermal energy in the sample (i.e., by annealing). As the strained alloy relaxes, the bond lengths and bond angles approach those of bulk $\text{Si}_{1-x}\text{Ge}_x$ (of corresponding composition). Because of the substrate influence, both strain and alloy composition must be considered when examining the properties of deposited $\text{Si}_{1-x}\text{Ge}_x$.

The goal of this study is to focus on the effects of composition on the atomic bonding in $\text{Si}_{1-x}\text{Ge}_x$ alloys. To separate the effects of composition and the effects of strain, relaxed $\text{Si}_{1-x}\text{Ge}_x$ films were used. In all the samples, except $\text{Si}_{0.64}\text{Ge}_{0.36}$, the thickness of the alloy layer deposited was greater than the critical thickness¹⁴ to en-

sure relaxation of the alloy. The $\text{Si}_{0.64}\text{Ge}_{0.36}$ sample was relaxed by repeated annealing. The $\text{Si}_{0.64}\text{Ge}_{0.36}$ sample was annealed *in situ* for 10 min at 400, 650, 700, and 750 °C. X-ray diffraction was used to examine the lattice parameters of the $\text{Si}_{1-x}\text{Ge}_x$ films to ensure that they were relaxed.

Alloy composition and thickness were measured by Rutherford backscattering (RBS). Rutherford backscattering analysis of the $\text{Si}_{1-x}\text{Ge}_x$ alloy films was carried out with 2.0-MeV He^+ ions. Samples were mounted on a computer-controlled two-axis goniometer; the rotational axis was perpendicular to the sample surface, and the tilt axis was in the surface plane of the sample and perpendicular to the beam direction. To increase the accuracy of the thickness and composition measurements the samples were tilted 50° from normal, away from the detector. The detector, with a narrow slit in front, was placed at a scattering angle of 165°. The Monte Carlo simulation program Win Spec¹⁵ was used to infer the thickness and composition of the $\text{Si}_{1-x}\text{Ge}_x$ alloy films.

The structural properties of the alloys were examined using x-ray diffraction (XRD) and extended x-ray-absorption fine structure (EXAFS). A Theta-2Theta goniometer with a Cu x-ray source was used for the XRD. A graphite monochromator rejected all x-ray energies except Cu K_α and K_β . The $\text{Si}(400)$ and $\text{Si}_{1-x}\text{Ge}_x(400)$ diffraction angles were measured, and the spacing of the $\text{Si}_{1-x}\text{Ge}_x(400)$ planes parallel to the alloy/substrate interface were calculated.

The EXAFS measurements were obtained at beamline X23A2 of the National Synchrotron Light Source (NSLS) at Brookhaven National Laboratory (BNL). All measurements were carried out at the germanium K absorption edge (11 103 eV). The electron-beam energy was either 2.53 or 2.58 GeV, with a stored current of between 100 and 245 mA. The x-ray energy was defined by a double-crystal monochromator with $\text{Si}(111)$ crystals. The energy calibration was periodically checked using a germanium foil in transmission. An electron yield detector with both sample tilt and rotation capabilities was used in a low angle configuration to minimize Bragg reflections. All samples were mounted in the same orientation to reduce differences in the data sets due to sample orientation beam polarization effects. Data was collected with the sample at room temperature. Increased integration times in the 381–975-eV region (above the absorption edge) were used to improve the signal-to-noise ratio of the EXAFS oscillations.

III. RESULTS

A. Strain

The measured lattice parameters (normal to the $\text{Si}_{1-x}\text{Ge}_x/\text{Si}$ interface) of the $\text{Si}_{1-x}\text{Ge}_x$ samples are plotted in Fig. 1. As mentioned previously, Vegard's law predicts that the lattice parameter of bulk $\text{Si}_{1-x}\text{Ge}_x$ will vary linearly with composition from the natural lattice constant of Si to the natural lattice constant of Ge.⁴ In a study of bulk $\text{Si}_{1-x}\text{Ge}_x$, Dismukes, Ekstrom, and Paff⁶ measured a downward bowing of the lattice parameter

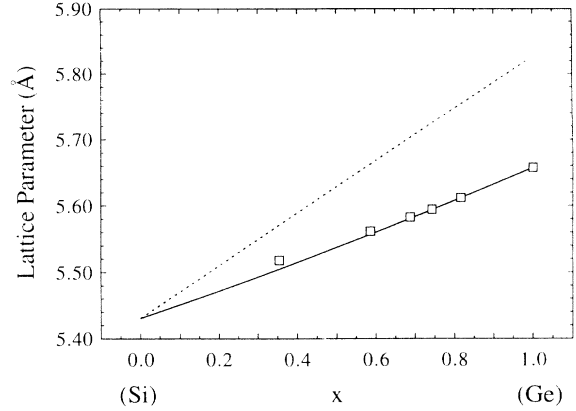


FIG. 1. $\text{Si}_{1-x}\text{Ge}_x$ lattice parameter, normal to the $\text{Si}_{1-x}\text{Ge}_x/\text{Si}$ interface, measured by XRD (open squares). Vegard's law with the bowing correction of Dismukes, Ekstrom, and Paff (Ref. 16) (solid line). The lattice parameters predicted for $\text{Si}_{1-x}\text{Ge}_x$ grown pseudomorphically on $\text{Si}(100)$ (dashed line).

away from Vegard's law. A maximum deviation of ~ 0.007 Å was observed for the Si-Ge lattice. Weidmann and Newman⁶ observed similar downward bowing when an exact solution was used in the relaxation of their supercell model. Analytical models of bulk $\text{Si}_{1-x}\text{Ge}_x$ which impose the condition of rigid neighbors during iterative supercell relaxation do not allow the lattice constants of the supercell to relax, and thus impose Vegard's law (i.e., lattice parameter bowing is not observed).⁶ To predict the bulk lattice parameter of the $\text{Si}_{1-x}\text{Ge}_x$ alloys used here, the deviations measured by Dismukes, Ekstrom, and Paff were modeled and added to lattice parameters predicted by Vegard's law. The lattice parameters predicted by this procedure are also plotted in Fig. 1 (solid line).

In Fig. 1 it can be seen that the measured lattice parameter of the $x=0.36$ sample is slightly larger than the lattice parameter predicted for bulk $\text{Si}_{0.64}\text{Ge}_{0.36}$. To determine if this deviation indicated a significant degree of residual biaxial compression, the lattice parameter of pseudomorphic (100% biaxially compressed) $\text{Si}_{0.64}\text{Ge}_{0.36}$ was estimated. In an analytical study of $\text{Si}_{1-x}\text{Ge}_x$ alloys by Xu¹⁷ it was predicted that the $\text{Si}_{1-x}\text{Ge}_x$ lattice parameter (normal to the surface) in alloys grown pseudomorphically on $\text{Si}(100)$ would vary linearly with alloy composition. The lattice parameter of Ge pseudomorphically grown on $\text{Si}(100)$ can be calculated using

$$a_p - a_{\text{Ge}} = -2(C_{12}/C_{11})(a_{\text{Si}} - a_{\text{Ge}}), \quad (2)$$

where a_p is the expanded Ge lattice parameter (normal to the surface), a_{Si} is the natural lattice constant of Si, a_{Ge} is the natural constant of bulk Ge, and C_{11} and C_{12} are the elastic constants of Ge ($C_{11}=1.32$ and $C_{12}=0.49$).¹⁸ The calculated value of the uniaxially expanded lattice parameter of Ge pseudomorphic on $\text{Si}(100)$ is 5.8260 Å. The expanded lattice parameter expected for $\text{Si}_{1-x}\text{Ge}_x$ grown pseudomorphically on $\text{Si}(100)$ is indicated by the dashed line in Fig. 1 which is a linear interpolation between the natural lattice constant of Si and the expanded

lattice parameter of pseudomorphic Ge. Using the estimated lattice parameter of pseudomorphic (100% biaxially compressed) $\text{Si}_{0.64}\text{Ge}_{0.36}$, it was determined that the residual biaxial compression in the $x=0.36$ sample was 20%. The residual biaxial compression was determined to be 4.6% in the $x=0.59$ sample and less than 1.5% in the remaining samples. The agreement of the measured lattice parameters with those predicted by the modified Vegard's law demonstrates that the alloy layers in this study are essentially completely relaxed and should exhibit bulklike properties.

B. Bond lengths

The EXAFS data sets used for analysis for each sample consisted of 3–6 EXAFS scans. The background subtraction portion of the MACXAFS3.1 analysis programs¹⁹ was used to isolate the EXAFS oscillations (χ data) of each scan and an average χ was calculated for each data set. The average χ from the data set of each sample was Fourier filtered and fitted to determine the atomic parameters of that sample. The forward and reverse Fourier-transform programs of the Eindhoven EXAFS analysis package were used to Fourier filter the EXAFS data to isolate the first shell data (Ge-Ge and Ge-Si bond-length information). The following parameters were used for Fourier filtering: k weight=2, transform k range=2.7–12.5 \AA^{-1} , and inverse transform R range=1.0–2.75 \AA (this gives $2\Delta R \Delta k / \pi = 10.9$ as an estimate of the number of free parameters).²⁰ The χ data and Fourier-filtered R -space data of the 59% Ge and Ge standard samples are shown in Figs. 2 and 3, respectively. During fitting the interatomic distance (R), occupancy (N), and disorder (σ^2) terms for both the Ge-Ge and Ge-Si components of the first shell were varied simultaneously. It was found that if the energy shift parameters (ΔE_{Si} , ΔE_{Ge}) were also allowed to vary independently the fitting produced ΔE 's, R 's, N 's, and σ 's which were clearly nonphysical. The energy shift parameters were set equal to a common value ($\Delta E_{\text{Si}} = \Delta E_{\text{Ge}} = \Delta E$). The value of ΔE was determined from the Ge standard.

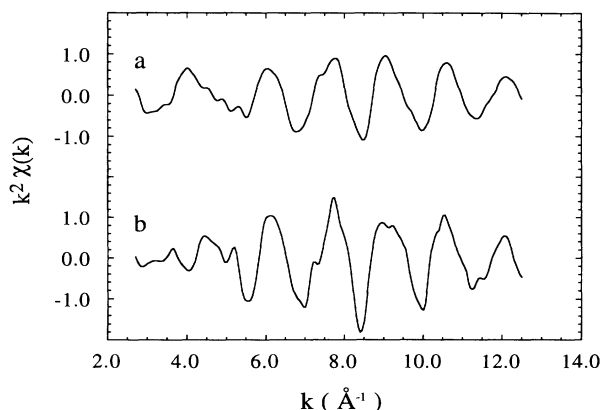


FIG. 2. EXAFS χ data of the $x=0.59$ sample (a) and the Ge standard sample (b) plotted with k weighting of 2. The Fourier-transform range of 2.7–12.5 \AA^{-1} , with k weighting of 2, was used for the subsequent Fourier filtering.

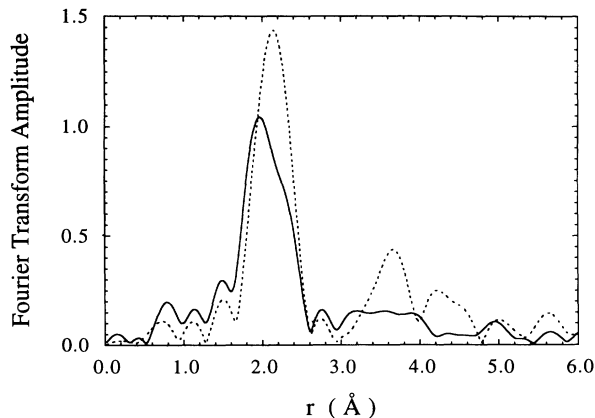


FIG. 3. Fourier-transformed EXAFS χ data for the $x=0.59$ sample (solid line) and the Ge standard sample (dashed line). The range of 1–2.75 \AA was used for the subsequent inverse Fourier transform (Fourier filtering).

Theoretical phase shift files generated by FEFF3.11 were used as references for the fitting.²¹ The Fourier-filtered first shell χ data and the best-fit results are plotted in Fig. 4 for the 59% Ge and Ge standard samples. The results of the EXAFS analysis are summarized in Table I.

C. Error analysis

The EXAFS data sets were collected during two separate experimental sessions at beamline X23A2 of the NSLS. A clean Ge(100) substrate, used as a germanium standard, was run during both sessions as a reference standard to check for systematic differences between the data from the two sessions. The only observed difference in the data from the two sessions was a slight (0.2) change in the average total coordination ($N_{\text{Si}} + N_{\text{Ge}}$). The consistency of the difference indicates that there was a systematic difference between the experiment and/or analysis of the two sessions. The composition of the $\text{Si}_{1-x}\text{Ge}_x$ alloy samples was calculated from the mea-

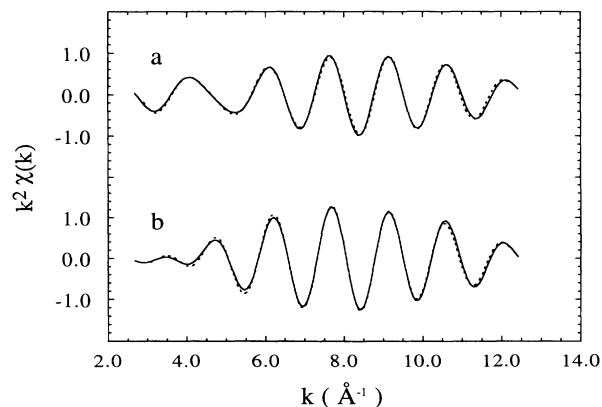


FIG. 4. The fitting results of the Fourier-filtered first shell data (Ge-Ge and Ge-Si bonds) of the $x=0.59$ sample (a) and pure Ge standard samples (b). The Fourier-filtered EXAFS χ data is indicated by the solid lines, and the best-fitting results are indicated by the dashed lines.

TABLE I. Results of Ge *K*-edge EXAFS analysis of $\text{Si}_{1-x}\text{Ge}_x$ samples and a pure Ge standard. Column 1: The Ge fraction x as determined by RBS. Column 2: The EXAFS data were collected during two separate experimental sessions and the run number indicates which samples were examined during each session. Columns 3 and 6: The number of Si and Ge nearest-neighbor atoms, respectively. Columns 4 and 7: The measured Ge-Si and Ge-Ge bond lengths, respectively. Columns 5 and 8: The Debye-Waller factors for the Gaussian disorder in the Ge-Si and Ge-Ge bond lengths, respectively. All six of the fitting parameters listed were allowed to vary during the fitting except as noted. The values denoted by (*) were held constant during the fitting. The value of $\Delta E0$ was held constant at -6.70 eV during the fitting.

Germanium				$\sigma_{\text{Ge-Si}}^2$			$\sigma_{\text{Ge-Ge}}^2$
fraction	Run		$R_{\text{Ge-Si}}$	(\AA^2)		$R_{\text{Ge-Ge}}$	(\AA^2)
(x)	No.	N_{Si}	(\AA)	$\times 10^{-4}$	N_{Ge}	(\AA)	$\times 10^{-4}$
0.36	1	2.7 ± 0.3	2.403 ± 0.010	46	1.6 ± 0.3	2.429 ± 0.011	37
0.59	2	1.7 ± 0.2	2.402 ± 0.014	44	2.4 ± 0.4	2.435 ± 0.007	42
0.69	1	1.4 ± 0.2	2.399 ± 0.013	47	3.0 ± 0.3	2.436 ± 0.005	48
0.74	1	1.2 ± 0.2	2.400 ± 0.018	44	3.2 ± 0.3	2.439 ± 0.005	47
0.82	2	0.8 ± 0.2	2.394 ± 0.040	45.2*	3.2 ± 0.7	2.442 ± 0.009	45.7*
Ge Std.	1&2				4.0*	2.4498*	47

sured Si and Ge coordinates ($x = N_{\text{Ge}} / [N_{\text{Si}} + N_{\text{Ge}}]$) and compared with the RBS composition measurements. The maximum difference between the two composition measurements was 0.02, which is within the error of both the EXAFS and RBS measurements. The small differences between the alloy compositions calculated by EXAFS and RBS indicates that the error effected the amplitudes of both the Ge-Ge and Ge-Si signals uniformly, independent of composition. The systematic shift in total coordination and the uniform way in which both the Ge-Ge and Ge-Si signals were affected suggests that there was a difference between the two sessions in either the orientation of the samples (polarization effect) or the normalization of the EXAFS χ data. The normalization factor is a multiplicative factor which affects the entire EXAFS scan uniformly (i.e., no k dependence), and errors in the normalization factors should only directly affect the total coordination. It is expected that the systematic differences in the total coordinations between the two runs have a negligible affect on the other parameters ($R, \sigma, \Delta E0$).

The EXAFS data collected from the Ge standard during both runs were fitted using known germanium parameters to determine the value of the energy shift parameter $\Delta E0$. The Ge-Ge bond length and coordination were held constant at the known values of 2.4498 \AA and 4, respectively. The σ and $\Delta E0$ parameters were allowed to vary as each of the EXAFS scans were fitted individually. From the fitting results the value of $\Delta E0 = -6.70 \pm 0.55$ eV was determined.

For the $\text{Si}_{1-x}\text{Ge}_x$ alloys the value of $\Delta E0$ was held constant at -6.70 eV, and the remaining six parameters were allowed to vary during the fitting. Allowing the N 's, R 's, and σ 's to vary during the fitting of the $\text{Si}_{0.18}\text{Ge}_{0.82}$ EXAFS data resulted in nonphysical values for the R 's and σ 's. The weighted mean values of $\sigma_{\text{Ge-Ge}}$ and $\sigma_{\text{Ge-Si}}$ were calculated from the fits of the other five $\text{Si}_{1-x}\text{Ge}_x$ samples, and the σ 's were held constant at these values during the fitting of the $\text{Si}_{0.18}\text{Ge}_{0.82}$ EXAFS data. The difficulty in fitting the $\text{Si}_{0.18}\text{Ge}_{0.82}$ EXAFS data is

reflected in the relatively large standard deviations calculated for the fit parameters of that alloy.

To estimate the standard deviations of the atomic parameters determined by EXAFS analysis, several sources of error were examined. During the EXAFS data fitting the "fit quality" was measured by the parameter $S^2 = \sum_i (\text{Exp}_i - \text{Model}_i)^2 W_i$ where the sum is over all the EXAFS data points, Exp_i are the EXAFS data points measured by experiment, Model_i are EXAFS data points calculated from a model using the fitting parameters, and W_i is a weighting function. The "best fit" was determined by allowing the fit parameters to vary such that S^2 was minimized. The fit quality parameter was found to be strongly dependent on some of the fitting parameters and weakly dependent on others. To determine the standard deviation of each fit parameter due to the fitting error and fitting sensitivity, the EXAFS fitting of each sample was repeated multiple times while each of the previously floated parameters were fixed at constant values. During the fittings the parameter being checked was fixed at constant values different from the best-fit value of the parameter, and the other fitting parameters were allowed to vary. The parameter being checked was increased above and decreased below its best-fit value until the fit quality parameter S^2 increased by 10%. A standard deviation was calculated from the maximum, minimum, and best-fit values of the parameter. The variances determined by this method were used as a starting point, and the variances caused by other sources of error were added in quadrature.

To determine the effect of noise on the variance of the fitting results, each EXAFS scan was analyzed individually. For each data set (i.e., for each sample) the χ data from the individual EXAFS scans were averaged together to reduce the random noise level. The average χ data were then processed and fitted and the results compared with the fitting results of the individual scans. From the comparison a variance, due to the random noise, was determined. To examine the effect of changes in the energy shift parameter $\Delta E0$, the fitting of each data set was

repeated two more times using energy shift parameters of -6.15 and -7.25 eV (i.e., -6.70 ± 0.55 eV). To examine the effect of data preprocessing (i.e., background subtraction and normalization) the preprocessing and fitting of several data sets were repeated several times using different preprocessing parameters each time. All of these errors were added to the fitting/sensitivity error to give an estimate of the total possible error in the EXAFS results. The error estimates appear in Table I along with the fitting results.

In a random $\text{Si}_{1-x}\text{Ge}_x$ alloy the relative contributions of the Ge-Ge and Ge-Si bonds to the total Ge *K*-edge EXAFS signal will be weighted by the alloy composition (e.g., for $\text{Si}_{0.2}\text{Ge}_{0.8}$ 80% of the Ge *K*-edge EXAFS signal will be due to the Ge-Ge bonds, and 20% will be due to the Ge-Si bonds). Assuming a constant noise level, the signal-to-total-noise ratio for the Ge-Ge and Ge-Si components will change with composition. As x approaches 1 the ratio of the signal to the total noise for the Ge-Si bond will decrease, and there will be a composition above which the signal-to-total-noise ratio is so low that the noise will cause instabilities in the fitting of the Ge-Si bond parameters. We believe this was the case for our $\text{Si}_{0.18}\text{Ge}_{0.82}$ sample. Numerous instabilities were encountered during the fitting of the EXAFS data of the $\text{Si}_{0.18}\text{Ge}_{0.82}$ sample. These instabilities led to the relatively large error bars on the Ge-Si bond length measured for that sample.

D. Calculation of the topological rigidity parameter a^{**}

Germanium *K*-edge EXAFS analysis can only measure the Ge-Ge and Ge-Si bond lengths in $\text{Si}_{1-x}\text{Ge}_x$ alloys. The definition of a^{**} [Eqs. (1)] predicts that the variation in the Ge-Ge, Ge-Si, and Si-Si bond lengths, as a function of composition, can be represented by three equivalently spaced parallel lines. At $x=1$ the Ge-Ge bond length will equal the natural Ge-Ge bond length (2.4498 Å), at $x=0$ the Si-Si bond length will equal the natural Si-Si bond length (2.3516 Å), and, as a consequence, at $x=0.5$ the Ge-Si bond length will equal the average of the natural Si-Si and Ge-Ge bond lengths (2.4007 Å). Thus, using the definition of a^{**} and the measured Ge-Ge bond lengths, it was possible to calculate the value of a^{**} and to predict the behavior of the Ge-Si and Si-Si bond lengths. A line was fitted to the measured Ge-Ge bond lengths and a value of $a^{**}=0.63$ was calculated for the topological rigidity parameter. By changing the slope of the line to the maximum and minimum limits allowed by the Ge-Ge bond-length error bars, the range of possible a^{**} values was determined to be $0.50 \leq a^{**} \leq 0.71$. Using this range of possible a^{**} values, theoretical Ge-Si bond lengths were calculated using Eq. (1) and compared with the measured Ge-Si bond lengths. The full range of theoretical Ge-Si bond lengths predicted by $0.50 \leq a^{**} \leq 0.71$ fell within the error of the measured Ge-Si bond lengths. The measured Ge-Ge and Ge-Si bond lengths and the theoretical Ge-Ge, Ge-Si, and Si-Si bond lengths predicted by $a^{**}=0.63$ are plotted in Fig. 5.

In EXAFS analysis there are often strong correlations between the EXAFS fitting parameters. Because the

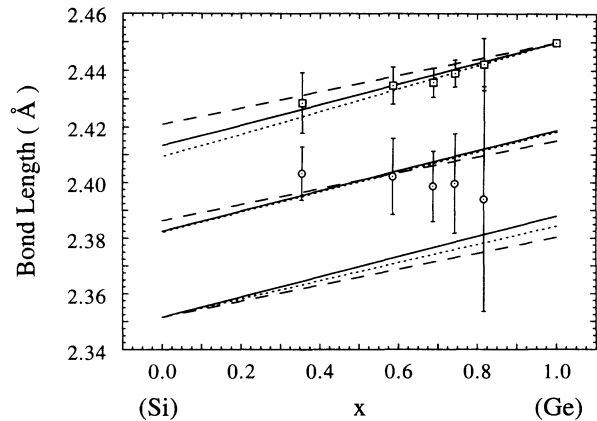


FIG. 5. Comparison of measured and predicted Ge-Ge and Ge-Si bond lengths in bulk $\text{Si}_{1-x}\text{Ge}_x$. The measured Ge-Ge and Ge-Si bond lengths are indicated by the open squares and open circles, respectively. The solid lines indicate the Ge-Ge, Ge-Si, and Si-Si bond lengths predicted by $a^{**}=0.63$. The renormalized predictions of Weidmann and Newman (Ref. 6) and Mousseau and Thorpe (Ref. 7) are indicated by the dotted and dashed lines, respectively. The predictions of Weidmann and Newman and Mousseau and Thorpe were based on natural Ge-Ge and Si-Si bond lengths different from the values assumed in this study (2.4498 and 2.3516 Å, respectively, for this study). For comparison the results of those studies were renormalized to the natural Ge-Ge and Si-Si bond lengths used in this study.

measured Ge-Si bond lengths do not fit well to $a^{**}=0.63$, it was necessary to check the correlation between the $R_{\text{Ge-Ge}}$ and $R_{\text{Ge-Si}}$ EXAFS fitting parameters (i.e., to determine if the $R_{\text{Ge-Si}}$ parameters were manipulated so that the $R_{\text{Ge-Ge}}$ parameters would match previous theoretical predictions). During the initial EXAFS data analysis both the $R_{\text{Ge-Ge}}$ and $R_{\text{Ge-Si}}$ parameters (and the N 's and σ 's) were allowed to vary (there are the results listed in Table I). To examine the correlation between the $R_{\text{Ge-Ge}}$ and $R_{\text{Ge-Si}}$ parameters the fitting of the EXAFS data was repeated two additional times, while the $R_{\text{Ge-Si}}$ parameter was held constant at arbitrary values. For each sample the fitting was repeated twice: once with $R_{\text{Ge-Si}}$ calculated from $a^{**}=1.00$ and once with $R_{\text{Ge-Si}}$ calculated from $a^{**}=0.63$. The Ge-Ge bond-length results of these constrained fits are plotted in Fig. 6. The maximum change in the measured Ge-Ge bond lengths caused by fixing the $R_{\text{Ge-Si}}$ values was 0.003 Å and the average change was 0.000 Å (zero). The Ge-Ge bond lengths from the first and second constrained fittings were used to calculate the values of $a^{**}=0.61$ and 0.62, respectively. These values are in very good agreement with the results of the initial EXAFS data analysis, indicating there is very little correlation between the $R_{\text{Ge-Ge}}$ and $R_{\text{Ge-Si}}$ fitting parameters.

IV. DISCUSSION

The renormalized theoretical results of Weidmann and Newman⁶ and Mousseau and Thorpe⁷ are also plotted in Fig. 5. Both of the theoretical predictions are in good agreement with the measured Ge-Ge bond lengths, and

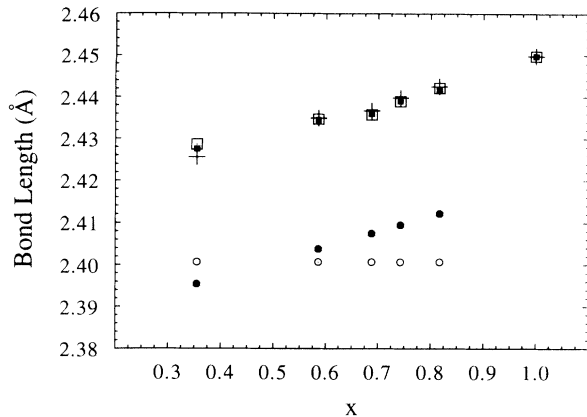


FIG. 6. Examination of the correlation between the EXAFS fitting parameters $R_{\text{Ge-Ge}}$ and $R_{\text{Ge-Si}}$. The Ge-Si bond lengths were predetermined, and the Ge-Ge bond lengths determined, from the EXAFS fitting. The open squares indicate the Ge-Ge bond lengths when $a^{**}=1.00$ was used to predetermine the Ge-Si bond lengths (open circles). The solid squares indicate the Ge-Ge bond lengths when $a^{**}=0.63$ was used to predetermine the Ge-Si bond lengths (solid circles). The crosses indicate the Ge-Ge bond lengths measured when both $R_{\text{Ge-Ge}}$ and $R_{\text{Ge-Si}}$ were allowed to vary during the EXAFS fitting. Only slight changes in the Ge-Ge bond lengths are seen, indicating that there is a low correlation between $R_{\text{Ge-Ge}}$ and $R_{\text{Ge-Si}}$.

are within the errors of the measured Ge-Si bond lengths. The experimental results of Kajiyama *et al.* suggested that the Ge-Ge, Ge-Si, and Si-Si bond lengths would not change with alloy composition. This appears to be plausible for the Ge-Si bond lengths we measured, but it clearly is not possible for the measured Ge-Ge bond lengths. Typically, in lieu of a complete error analysis, error bars of ± 0.02 Å are assigned to bond lengths determined by EXAFS analysis. Since no bond-length error bars were quoted by Kajiyama *et al.*, we arbitrarily assigned the bond-length error of ± 0.02 Å to their results. Using the bond-length measurements of Kajiyama *et al.* and the arbitrary ± 0.02 -Å error bars, we calculated the possible range of the topological rigidity parameter to be $0.69 \leq a^{**} \leq 1.00$. The lower limit of this range ($a^{**}=0.69$) is within the error of our bond-length measurements and is at the upper limit of the predictions of the analytical models, suggesting that the results of Kajiyama *et al.* may not actually be in conflict with the analytical models and the results of this study. The real error bars on the measurements of Kajiyama *et al.* may actually encompass the bond-length measurements of this study and the predicted bond lengths of the VFF-based analytical models.

Another possible explanation for the bond-length measurements of Kajiyama *et al.* comes from an analytical study by Mousseau and Thorpe.²² The samples used in the study by Kajiyama *et al.*¹⁰ were prepared by chemical-vapor deposition (CVD) of amorphous $\text{Si}_{1-x}\text{Ge}_x$ on polycrystalline graphite with subsequent annealing to crystallize the alloy. Mousseau and Thorpe²² modeled the effects of H trapped in $\text{Si}_{1-x}\text{Ge}_x$ on the Ge-Ge, Ge-Si, and Si-Si bonding. They determined that the

presence of significant levels of hydrogen would cause the remaining Ge-Ge, Ge-Si, and Si-Si bonds to relax closer to their natural values, thus reducing the effect of composition on the bond lengths (making the lattice less rigid and increasing the topological rigidity parameter). The trends in the experimental results of Kajiyama *et al.*¹⁰ are in good agreement with the analytical model of bond lengths in polycrystalline $\text{Si}_{1-x}\text{Ge}_x:\text{H}_y$ of Mousseau and Thorpe.²²

The values of a^{**} calculated from the results of this study and calculated from the results of VFF-based analytical studies fall in the range of $0.50 \leq a^{**} \leq 0.71$, indicating a combination of Bragg-Pauling- and Vegard-type behaviors. A similar mixture of Bragg-Pauling- and Vegard-type behaviors has been predicted for other semiconductor alloy systems. In the analytical study by Martins and Zunger,⁵ a parameter ϵ was defined for ternary alloys such that $\epsilon=1$ indicates Bragg-Pauling-type behavior and $\epsilon=0$ indicates Vegard-type behavior. They examined 64 binary and ternary semiconductor alloy systems, and found that ϵ was in the range 0.6–0.8 for most of the semiconductors considered. Their results predict that the behaviors of most semiconductor systems are a combination of Bragg-Pauling- and Vegard-type behaviors and are closer to the Bragg-Pauling limit ($\epsilon=1$) than to the Vegard limit ($\epsilon=0$). This type of bonding behavior has been observed, by EXAFS, in other semiconductor systems. Mikkelsen and Boyce¹ examined the In-As and Ga-As bond lengths in $\text{Ga}_{1-x}\text{In}_x\text{As}$ solid solutions. They measured a change in both bond lengths of ≈ 0.038 Å across the alloy composition range. Martins and Zunger⁵ calculated $\epsilon \approx 0.78(6)$ for the $\text{Ga}_{1-x}\text{In}_x\text{As}$ system, and we calculated $a^{**} \approx 0.78(6)$ from the results of Mikkelsen and Boyce.¹

V. CONCLUSIONS

We have shown that in relaxed MBE-deposited crystalline $\text{Si}_{1-x}\text{Ge}_x$ alloys, the effects of composition on atomic bonding are the same as predicted for bulk $\text{Si}_{1-x}\text{Ge}_x$ alloys. Heteroepitaxial $\text{Si}_{1-x}\text{Ge}_x$ alloys were grown on clean Si(100), and the levels of strain in the alloys were measured to insure that the alloys had relaxed. We have used germanium *K*-edge EXAFS analysis directly to measure the Ge-Ge and Ge-Si bond lengths in the $\text{Si}_{1-x}\text{Ge}_x$ alloys. Valence force field (VFF)-based analytical models of bulk $\text{Si}_{1-x}\text{Ge}_x$ alloys predict that the Ge-Ge, Ge-Si, and Si-Si bonds maintain distinctly different lengths which vary linearly with alloy composition.^{5–7} The measured Ge-Ge and Ge-Si bond lengths were in good agreement with those predictions. The topological rigidity parameter a^{**} was used to quantify the linear dependence of the bond lengths on alloy composition. From the measured Ge-Ge and Ge-Si bond lengths a value of $a^{**}=0.63^{+0.08}_{-0.13}$ was determined. The value of $a^{**}=0.63$ indicates that the bonding in $\text{Si}_{1-x}\text{Ge}_x$ exhibits both Bragg-Pauling-type and Vegard-type behaviors (i.e., both bond lengths and bond angles respond to the strain of mismatched bond lengths). The results of previous EXAFS studies which apparently conflict with the analytical

models may be explained in terms of hydrogen incorporation in the $\text{Si}_{1-x}\text{Ge}_x$ alloy lattice.^{10,22}

ACKNOWLEDGMENTS

The authors would like to thank Dr. Kathie Newman and Evert Vandeworp of Notre Dame University and Dr. Carl Foiles of Michigan State University for valuable discussions and comments regarding atomic bonding in $\text{Si}_{1-x}\text{Ge}_x$ alloys. The authors would like to thank Dr. Michael Thorpe of Michigan State University for his

helpful suggestions and comments during the EXAFS data analysis and for his critical review of this manuscript. The authors would also like to thank Kiyotaka Ishibashi for his RBS analysis at the University of North Carolina. This work was supported in part by the Division of Materials Science of the Department of Energy under Contract No. DE-FG05-89ER45384. R.J.N. acknowledges support by the National Science Foundation through Grant No. DMR 9204285. Beamline X23A2 of the National Synchrotron Light Source at Brookhaven National Laboratory is supported in part by the National Institute of Standards and Technology.

¹J. C. Mikkelsen, Jr. and J. B. Boyce, *Phys. Rev. B* **28**, 7130 (1983).

²W. L. Bragg, *Philos. Mag.* **40**, 169 (1920).

³L. Pauling, *The Nature of the Chemical Bond* (Cornell University Press, Ithaca, NY, 1967).

⁴L. Vegard, *Z. Phys.* **5**, 17 (1921).

⁵J. L. Martins and A. Zunger, *Phys. Rev. B* **30**, 6217 (1984).

⁶M. R. Weidmann and K. E. Newman, *Phys. Rev. B* **45**, 8388 (1992).

⁷N. Mousseau and M. F. Thorpe, *Phys. Rev. B* **46**, 15 887 (1992).

⁸Y. Cai and M. F. Thorpe, *Phys. Rev. B* **46**, 15 872 (1992).

⁹S. de Gironcoli, P. Giannozzi, and S. Baroni, *Phys. Rev. Lett.* **66**, 2116 (1991).

¹⁰H. Kajiyama, S. Muramatsu, T. Shimada, and Y. Nishino, *Phys. Rev. B* **45**, 14 005 (1992).

¹¹H. Jeon, C. A. Sukow, J. W. Honeycutt, T. P. Humphreys, R. J. Nemanich, and G. A. Rozgonyi, in *Advanced Metallizations in Microelectronics*, edited by A. Katz, S. P. Murarka, and A. Appelbaum, MRS Symposia Proceedings No. 181 (Materials

Research Society, Pittsburgh, 1991), p. 559.

¹²J. C. Bean, in *Proceedings of the First International Symposium on Silicon Molecular Beam Epitaxy*, edited by J. C. Bean (Electrochemical Society, Pennington, NJ, 1985), p. 337.

¹³R. People, *IEEE J. Quantum Electron* **22**, 1696 (1986).

¹⁴R. Hull, J. C. Bean, D. J. Eaglesham, J. M. Bonar, and C. Buescher, *Thin Solid Films* **183**, 117 (1989).

¹⁵E. Frey and N. Parikh, computer code Win Spec (University of North Carolina, Chapel Hill, NC, 1988).

¹⁶J. P. Dismukes, L. Ekstrom, and R. J. Paff, *J. Phys. Chem.* **68**, 3021 (1964).

¹⁷Z. Xu, *J. Phys. Condens. Matter* **5**, 9077 (1993).

¹⁸S. Wie, D. C. Allan, and J. W. Wilkins, *Phys. Rev. B* **46**, 12 411 (1992).

¹⁹C. Bouldin, *Comput. Phys.* (to be published).

²⁰F. W. Lytle, D. E. Sayers, and E. A. Stern, *Physica B* **158**, 701 (1989).

²¹J. Mustre de Leon, J. J. Rehr, S. I. Zabinsky, and R. C. Albers, *Phys. Rev. B* **44**, 4146 (1991).

²²N. Mousseau and M. F. Thorpe, *Phys. Rev. B* **48**, 5172 (1993).